RSC Advances

ROYAL SOCIETY OF CHEMISTRY

www.rsc.org/advances

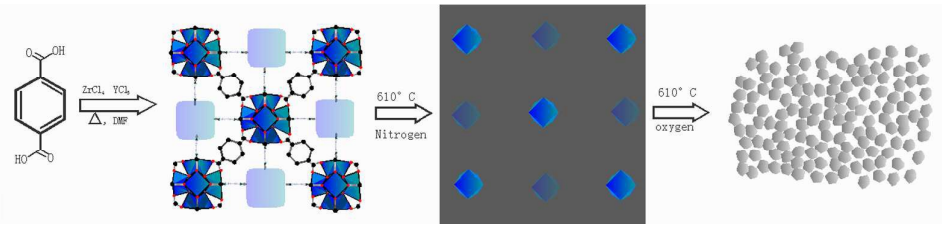

Mesoporous yttria stabilized zirconia (YSZ) with single cubic structures is obtained via two-step thermal treatment based on Y-doped UiO-66 template.

Cite this: DOI: 10.1039/c0xx00000x

www.rsc.org/xxxxxx

ARTICLE TYPE

Yttria stabilized zirconia derived from metal-organic frameworks

Zifeng Yue, Shucheng Liu, and Yi Liu*

Received (in XXX, XXX) Xth XXXXXXXXX 20XX, Accepted Xth XXXXXXXXX 20XX
DOI: 10.1039/b000000x

By choosing Zr(Y) based metal organic frameworks (MOFs) as a precursor and porous template, mesoporous yttria stabilized zirconia (YSZ) was synthesized using a simple thermal treatment. The green YSZ derived from such MOFs exhibits both high specific surface area and oxygen ion conductivity. This MOF-based method provides a new approach to the controllable synthesis of zirconia electrolytes.

1.Introduction

Due to its high oxygen ion conductivity, yttria stabilized zirconia (YSZ) has been widely used in many fields as a catalyst, sensor, adsorbent, and electrolyte in solid oxide fuel cells (SOFC).[1-3] Traditionally, YSZ was produced using solid-state reaction processes, hydrothermal treatments, thermal decomposition, or sol–gel strategies based on the hydrolysis of metal alkoxides. Recently, the fabrication of meso-structured YSZ has become extremely important for applications where high surface areas are required, for example, SOFC electrodes. Its high porosity and thermal stability significantly improves fuel/oxidant mass transport, oxide ion mobility, electronic conductivity, and charge transfer in the triplephase-boundary region (TPB) of SOFC electrodes.[4] Mesoporous YSZ has typically been obtained using hard-templating and surfactant based self-assembly techniques.[5-8] However, these synthesis routes require strict monitoring of experimental conditions, and the structures collapse immediately upon removal from the surfactant.

Porous metal organic frameworks (MOFs) constructed from metal ions and organic ligands have received much attention over the past few years.[9-11] Owing to their open channels, permanent cavities, and ordered crystalline lattices, MOFs offer great potential as self-sacrificing templates in the preparation of porous oxides.[12-15] Metal oxide clusters in MOFs can be converted into nanostructural metal oxides under heated conditions, and the carbogenic formed by the thermal decomposition of ligands acts as a barrier, preventing the oxide particles from agglomerating. Because of their porosity, high specific surface area, and easily removable features, MOFs possess unique advantages compared to other templates.

In this paper, we develop a novel and simple MOF route for preparing mesoporous YSZ with nanocrystalline frameworks, the process of which involves converting Zr-O and Y-O secondary building units (SBUs) into mesoporous oxides using a two-step calcination treatment. Here, we selected Zr-based UiO-66 MOFs as the initial precursor. These UiO type MOFs are based on a

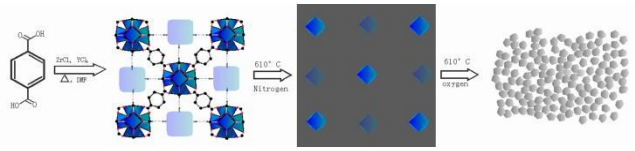

Scheme 1 Schematic representation of formation of yttria stabilized zirconia from MOFs via two-step calcination treatment

$(Zr)_6O_4(OH)_4$ octahedron SBU, where each zirconium metal center connects to 12 benzene-1,4-dicarboxylate (BDC) linkers to form a 3D framework.[16,17] Y^{3+} ions are incorporated into the UiO-66 framework during solvothermal crystallization. Some of the zirconium ions that form the inorganic clusters of UiO-66 are replaced by yttrium ions. As a result, the yttrium doped UiO-66 template contains integrated Zr-O and Y-O clusters. During thermal decomposition in an inert atmosphere, the metal ions in the MOFs are transformed into ZrO_2 (Y_2O_3) nanoparticles, and the organic ligands are converted into carbonaceous structures. Finally, upon thermolysis in oxygen, the confined carbogenic evaporates, generating highly porous nanocrystalline YSZ. A schematic view of this synthesis is shown in Scheme. 1.

2. Experimental section

Y-doped UiO-66 was prepared using a solvothermal method. An appropriate amount of zirconium chloride ($ZrCl_4$), 1,4-benzenedicarboxylic acid (H_2BDC), yttrium chloride (YCl_3) and N,N-dimethyformamide (DMF) were mixed in a 50 ml Teflon-lined stainless steel autoclave and heated at 120 ℃ for 60 hours. The Y/Zr ration (8%，30%，50% in mole）was controlled by using different amounts of $ZrCl_4$ and YCl_3. The product was cooled to room temperature, then filtered and washed three times with DMF. Excess H_2BDC and DMF in the pores of materials were removed using a heat treatment at 300 ℃ for 24 hours.The as-made MOF crystal was calcined in two-steps, first in a tube furnace under a N_2 atmosphere and then in an O_2 atmosphere at 610 ℃. The final products were designated 8YSZ, 30YSZ, and 50YSZ, respectively. To obtain electrical measurements, the YSZ powders were uniaxially pressed into pellets under a pressure of 900 MPa. Then silver paste was applied to the surface of the pellet and it was heated at 180 ℃ for 10 min.

3. Results and discussion

The crystal structures of the MOF templates were measured using wide-angle X-ray diffraction (XRD), as shown in Fig. 1(a). The

relative intensity and peak positions found in the XRD pattern is consistent with previous reports[16], confirming the formation of desirable UiO type crystalline frameworks. The XRD patterns of

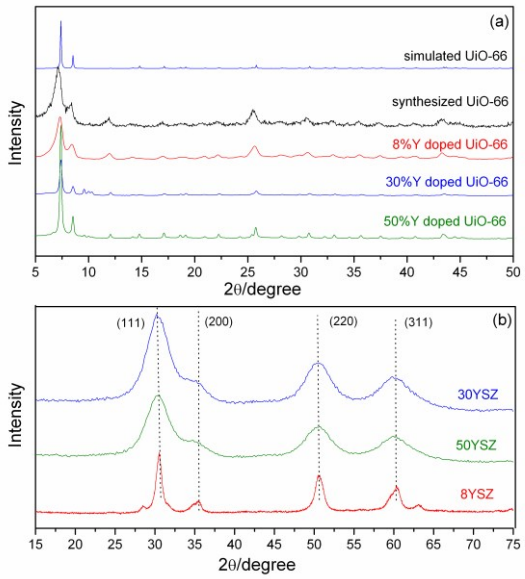

Fig. 1 PXRD patterns of samples: (a) UiO-66 and Y-doped UiO-66; (b) YSZ derived from Y-doped UiO-66

the synthesized YSZ are shown in Fig. 1(b). It was observed that both samples had four diffraction peaks occurring at 2θ=30.4°, 35.3°, 50.7°, and 60.4°, which correspond to the (111), (200), (220), and (311) lattice planes of the fluorite type cubic zirconia. (JCPDS card No.30-1468)

The morphology, microstructures, and porous characteristics of the samples were examined using SEM, TEM and HRTEM. The SEM images of the synthesized YSZ (Fig. S2) exhibit a porous structure. Fig. 2a shows the SEM images of the 30YSZ green powder, which shows that wormhole-like zirconia was prepared. Close inspection reveals that particles with diameter of about 50 nm cohered together to form a skeleton. As shown in the TEM images (Fig. 2b, 2c), the YSZ materials exhibit a spindle morphology that is comprised of highly nanoporous structures. The HRTEM images, shown in Fig. 2d, clearly reveal the presence of nonaggregated nanocrystalline particles in the YSZ composites. A clear lattice pattern is visible, indicating the high crystallinity of the YSZ particles present in the composites.

In order to explore the formation mechanism of the oxides derived from the MOFs, we studied MOF degradation using thermo-gravimetric (TG) analysis, as is shown in Fig. S1. The guest water and the solvent molecules that occupied the voided spaces of the MOFs were removed by heating the structures from room temperature to 200℃. Weighing the MOFs, it was discovered that they had lost 40% of their weight during the second step of the calcination process. This loss was ascribed to the decomposition of the MOF framework occurring at temperatures ranging from 500 to 700℃.

The chemical state of yttria stabilized zirconia was investigated using X-ray photoelectron spectroscopy (XPS) to probe the properties of the inner-shell electrons. A wide scan survey spectrum (Fig. S3-5a) identified the elemental composition of the sample. High-resolution narrow-scan spectra were obtained and peak deconvolutions performed for the O1s, Y1s, and Zr3d core levels. The O1s spectrum (Fig. S3-5b) reveals only one peak at 529.8 eV, which can be attributed to the O in YSZ. The two peaks at 181.8 and 184.1eV in the Zr3d spectrum (Fig. S3-5c) can be ascribed to the spin-orbit splitting of the Zr3d components, Zr3d5/2 and Zr3d3/2. The observed Zr 3d5/2 BEs of ~181 eV for the samples are higher than that of metallic Zr (178.7-180.0 eV), ZrC (178.6−179.6 eV), but comparable to that of ZrOx ($0 < x < 2$, 180.8-181.4 eV).[18,19] Therefore, it can be concluded that the Zr

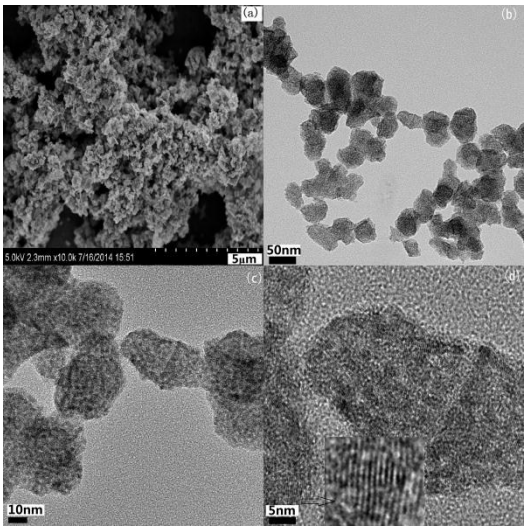

Fig.2 SEM image (a); TEM image (b,c); and HRTEM image (d) of 30YSZ

atoms in the composites are primarily in the oxidation state. The Y3d spectrum (Fig. S3-5d) shows a peak at 158.5 eV, which can be attributed to the oxidation state of yttrium.

The N_2 adsorption-desorption isotherm and the Barrett-Joyner-Halenda (BJH) adsorption pore size distribution plot of the as-prepared YSZ are shown in Fig. S6. The curves of the samples adhere to the type-IV isotherm with a pronounced hysteresis loop, a typical characteristic of mesoporous adsorbents. The inset in Fig. S6 shows that, according to the BJH model, the samples have relatively broad, mico- to meso-pore-sized diameters. The average diameters of pores on the 8YSZ, 30YSZ, and 50YSZ MOFs were calculated to be 20.9 nm, 34.6 nm, and 21.8 nm, respectively. The specific BET surface area and total pore volume of the as-prepared 8YSZ, 30YSZ, and 50YSZ MOFs was measured to be 33.2 m^2g^{-1}(0.17 cm^3g^{-1}), 25.7 m^2g^{-1}(0.22 cm^3g^{-1}), and 16.5 m^2g^{-1}(0.09 cm^3g^{-1}), respectively. We think that the surface area of the final YSZ come from the internal and external surface of single YSZ particle, as well as void lies in between particles.

AC impedance spectra of the YSZ green disks without sintering at high temperature are shown in Fig. 3. The complex-impedance plane plots were fitted using two depressed and overlapping semi-circular arcs corresponding to grain interior and grain boundary contributions. The fitted parameters were used to estimate oxygen ion conductivity and activation energies. The total conductivity was calculated using the conventional relationship σ=L/AR, where R is the total resistance determined

from the fitting of the impedance diagrams, L is the thickness of the sample under study, and A is its geometric area. It was observed that the YSZ green disks derived from Y-doped UiO-66 exhibit a relatively high ionic conductivity. At 500 ℃, the total conductivity of the 50YSZ green disks was determined as 1.74×10^{-6} S cm^{-1}. This conductivity was found to be much higher than that of a green disk of pure zirconia at the same temperature. Moreover, 50YSZ demonstrated much higher conductivity than other samples, indicating that the transformation of the SBUs to oxides on Y-doped UiO-66 causes a steep increase in conductivity due to the increased concentration of oxygen vacancies. As is known, Y^{3+} dissolved into ZrO_2 can create oxygen vacancies because the substitution of Zr^{4+} for Y^{3+} causes a negative net charge in the lattice such that the charge neutrality condition can only be maintained by the formation of oxygen

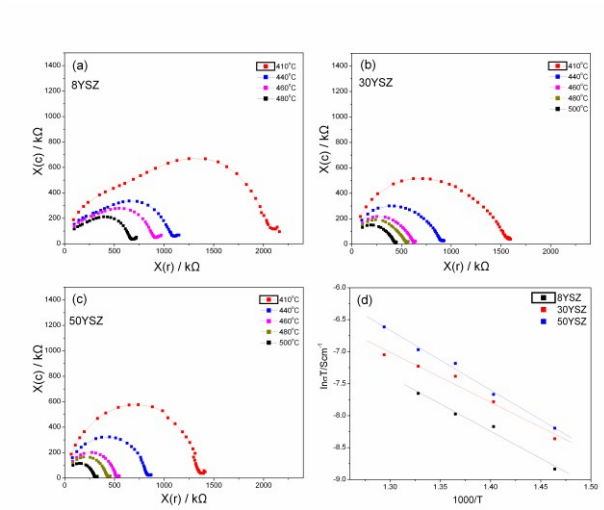

Fig.3 AC impedance spectra (a-c) and Arrhenius curves(d) of yttria doped zirconia

vacancies. It is expressed as follows:

$$Y_2O_3 \xrightarrow{ZrO_2} 2Y_{Zr}^{'} + V_{\ddot{O}} + O_O^{\times},$$

Where $Y_{Zr}^{\prime}$ denotes the Y in the Zr sites with the apparent negative charge, and $V_{\ddot{O}}$ is the vacancy in the oxygen sites with a double positive charge. $O_O^{\times}$ is the lattice oxygen, i.e., the oxygen in the oxygen sites with net charge of zero. Oxygen is transported by hopping through its vacancy sites, and the concentration of oxygen vacancy is determined by the concentration of the yttrium dopant. In Y-doped UiO-66, the Zr(Y)-O SBU is constructed of six zirconium (yttrium) cations, which form an octahedron. Each SBU is connected to twelve other SBUs by dicarboxylate linkers. Annealing the MOFs in an inert atmosphere, the ZrO_2 and Y_2O_3 particles embed into the carbon matrix in situ. After being subsequently sintered in oxygen, the carbon matrix evaporates, and ZrO_2 reacts with Y_2O_3 to create oxygen vacancies for charge compensation.

The conductivity as a function of temperature is derived from the Arrhenius equation, expressed as follows:

$$\sigma = \frac{\sigma_0}{T}\exp-\frac{E_a}{kT}$$

Where σ_0 is the pre-exponential factor, T is the absolute temperature, k is the Boltzmann constant, and Ea is the activation energy of the process, including sum of the migration and dissociation energy of vacancies. Fig. 3d shows the total conductivity plotted according to the Arrhenius law. The curves show the linear trend typically observed in ceramic samples. The activation energies of 0.73eV, 0.67eV, and 0.80eV were determined for the 8YSZ, 30YSZ, and 50YSZ, respectively. The relatively low activation energy indicates low migration enthalpy of oxygen vacancies given that the formation of vacancy clusters and the defect interactions will affect activation energy and conductivity in polycrystalline YSZ. These interactions among the defects have been described as dipoles and tripoles and denoted as $[Y_{Zr}^{\prime}-V_{\ddot{O}}]^{\cdot}$ and $[Y_{Zr}^{\prime}-V_{\ddot{O}}-Y_{Zr}^{\prime}]^{\times}$ respectively.[20] The low activation energy in these samples showed that oxygen ion transport occurs through vacancies whose nearest neighbor is a Zr^{+4} ion, meaning that tripole type vacancies do not contribute to conductivity.[21] Typically, tripole type defects are formed during the condensation process of sintering. However, in this work, we used green powder which was pressed into pellets under a pressure of 900 MPa for electric measurement, which enabled the porous structure of the sample to be maintained and the defect interactions to decrease. Thus, the migration of oxygen vacancies is more efficient in the MOF-derived sample.

4. Conclusion

In summary, we report a new strategy for controllable synthesis of YSZ by using Y-doped UiO-66 as a template. Pure YSZ with single cubic structures are obtained via two-step thermal treatment. These mesoporous materials have large surface areas, crystalline frameworks, and high oxygen ion conductivity, which is advantageous for application in SOFC electrodes. By designing the Y/Zr ratio in the SBUs of the MOFs, we could readily control the yttria stabilizer amount in the zirconia. It is expected that this MOF-directed template method will provide new opportunities for rational design and synthesis of other zirconia based electrolytes through the use of functional MOFs.

Acknowledgements

This work was supported by the National Natural Science Foundation of China (21261006), Natural Science Foundation of Guizhou province (2012/2115) and Graduate Innovation Fund of Guizhou University (2014069).

Notes and references

College of Science, Guizhou University, Guiyang 550025, China
E-mail: sci.yiliu@gzu.edu.cn

† Electronic Supplementary Information (ESI) available: [details of any supplementary information available should be included here]. See DOI: 10.1039/b000000x/

1 A. Pimenov, J. Ullrich, P. Lunkenheimer, A. Loidl and C.H. Ruscher, *Solid State Ion*, 1998, **109**,111.
2 T.S.Zhang, S.H.Chan, W.Wang, K.Hbaieb, L.B.Kong and J.Ma, *Solid State Ion*, 2009,**180**, 82.
3 N.H.Perry and T.O.Mason, *Solid State Ion*, 2010,**181**,276.
4 M. Mamak, N.Coombs and G.Ozin, *J Am Chem Soc*, 2000, **122**, 8923.
5 H.R.Chen, J.L.Gu, J.L.Shi, Z.L.Liu, J.H.Gao and M.L.Ruan, *Adv Mater*, 2005,**17**,2010
6 M.S.Wong and J.Y.Ying, *Chem Mater*, 1998 ,**10**,2067.

7 F. Ma, J.H. Sun, H.J. Zhao, Y.Li and S.J.Luo, *Stud Surf Sci Catal*, 2007, **165**,301.
8 H.R.Chen, J.L.Shi, W.H.Zhang, M.L.Yuan and D.S.Yan, *Chem Mater* 2001, **13**,1035.
9 H.Li, M.Eddaoudi and M.O'Keeff, Nature,1999,**402**,276.
10 K.L.Mulfort, J.T.Hupp, *J Am Chem Soc*, 2007,**129**,9604.
11 N. Stock and S.Biswas, *Chem Rev*, 2012,**112**,933.
12 K.E.Dekrafft, C.Wang and W.B.Lin, *Adv Mater* 2012,**24**,2014.
13 R.B.Wu, X.K.Qian, F.Yu, H.Liu, K.Zhou and J.Wei, *J Mater Chem A* 2013,**1**,11126.
14 T.K.Kim, K.J.Lee, J.Y.Cheon, J.H.Lee, S.H.Joo and H.R.Moon, *J Am Chem Soc* ,2013,**135**,8940.
15 L.Peng, J.L.Zhang, Z.M.Xue, B.X.Han, J.S.Li and G.Y.Yang, *Chem Commun*,2013,49,11695.
16 J.H.Cavka, S.Jakobsen, U.Olsbye, N.Guillou, C.Lamberti, S.Bordiga and K.P.Lillerud, *J Am Chem Soc*, 2008 ,**130**, 13850.
17 S.A.Steiner, T.F.Baumann, B.C.Bayer, R.Blume, M.A.Worsley, W. J.MoberlyChan, E.L.Shaw, R.Schlogl, A.J.Hart, S.Hofmann and B. L.Wardle, *J Am Chem Soc*, 2009, 131, 12144.
18 Y. M.Wang, Y.S.Li, P.C.Wong and K.A.R.Mitchell, *Appl. Surf.Sci*, 1993, **72**, 237.
19 T.L.Barr, *J Phys Chem B*, 1978, **82**, 1801.
20 A.R.Haering and H.Schichl, *Solid State Ion*, 2005,**176**,253.
21 J.Khare,M.P.Joshi, S.Satapathy, H.Srivastava and L.M.Kukreja, *Ceram Inter*, 2014,**40**,14677.

